Sakarya Üniversitesi Fen Bilimleri Dergisi
Sakarya University Journal of Science

e-ISSN : 2147-835X
Publisher : Sakarya University

Vol. 29, No. 4, 402-425, 2025
DOI: https://doi.org/10.16984/saufenbilder.1713546

Research Article

Evaluation of Thermal Transfer Efficiency and Nonlinear Shear Effects on Flow Modulation in a Flexible Microfluidic Heat Transfer System

Uchenna Uka[1*], Edwin Esekhaigbe[2], Joseph Emegha[3], Godswill Kalu[4]

[1] Babcock University, School of Science and Technology, Department of Basic Sciences, Ilishan-Remo, Ogun State, Nigeria, ukau@babcock.edu.ng, ror.org/00k0k7y87
[2] University of Africa, Faculty of Science, Department of Mathematics and Computer Sciences, Tru-Orua, Bayelsa State, Nigeria, steadystatesolution@gmail.com, ror.org/04xrk2k91
[3] Hensard University, Faculty of Computer Science and Computing, Bayelsa State, Nigeria, jjjemegha@yahoo.com
[4] Rivers State University, Faculty of Engineering, Department of Mechanical Engineering, Oroworukwo, Port Harcourt, Nigeria, kgodswill@yahoo.com, ror.org/01kr7aq59
[*]Corresponding Author

ARTICLE INFO

Keywords:
Inclination
Kinetic effect
MHD
RK4
Viscous dissipation

Article History:
Received: 04.06.2025
Revised: 29.07.2025
Accepted: 31.07.2025
Online Available: 11.08.2025

ABSTRACT

This study examines the thermal transfer performance of a microfluidic heat transfer system, with a focus on the interplay between flow orientation, flexibility, and nonlinear shear dilution/enhancement effects. A mathematical model was developed to describe the heat transfer dynamics within a flexible microchannel subjected to Robin boundary conditions, accounting for complex flow behaviors. The governing partial differential equations (PDEs) were transformed into a system of coupled ordinary differential equations (ODEs) using appropriate similarity quantities, the fourth-order Runge-Kutta-Fehlberg method, and shooting techniques to facilitate efficient computation of thermal, mass, and flow distributions. Subsequently, Maplesoft 16 was used to simulate the resulting system of equations. The analysis explores how flow orientation influences shear-induced dilution or enhancement, impacting effective thermal conductivity and heat transfer efficiency. The flexibility of the microchannel walls introduces nonlinear effects, modulating the flow profile and heat dissipation rates. Results indicate that optimal flow orientation and controlled flexibility significantly enhance thermal performance, with nonlinear shear effects amplifying or mitigating heat transfer depending on the flow regime. These findings provide valuable insights for designing advanced microfluidic systems for applications requiring precise thermal management, such as microelectronics cooling and lab-on-chip devices. Additionally, the Nusselt number decreases as the Prandtl number increases, while the Sherwood number rises due to an enhanced Schmidt number.

1. Introduction

Elevated levels of thermal movement in engineering, biochemical, and medical miniature systems require thermal converters that are compact, lightweight, and highly effective. Tiny conduits, made from transparent materials, semiconductors, or synthetic compounds, form the core components of these miniature systems. To enhance the thermal efficiency of small-scale devices, superior cooling agents are needed compared to traditional liquids, such as lubricants, water (H_2O), or antifreeze compounds. One approach to addressing a small-scale refrigeration challenge is to incorporate dense nanoscale particles into the liquid. These nano-enhanced liquids, specifically thin dispersions of nanoscale particles in fluids, significantly alter the mixture's properties, particularly its heat transmission and viscosity.

Nanoscale particles evaluated for miniature system refrigeration range from metallic elements and compounds to carbon-based

Cite as: U. Uka, E. Esekhaigbe, J. Emegha, G. Kalu, "Evaluation of thermal transfer efficiency and nonlinear shear effects on flow modulation in a flexible microfluidic heat transfer system," Sakarya University Journal of Science, vol. 29, no. 4, pp. 402-425, 2025. https://doi.org/10.16984/saufenbilder.1713546

microtubes measuring 1–100 nanometers. Laboratory evidence consistently indicates a greater improvement in the thermal conductivity of nano-enhanced liquids (k_{nf}) as predicted by Maxwell's "functional medium" model [1] or the Hamilton and Crosser model [2]. This increase in k_{nf} compared to the base liquid's thermal conductivity (k-base-liquid) varies with factors such as nanoparticle proportion, size, shape, material, surface electrical charge, degree of particle clustering, type of base liquid, temperature, electrical conductivity, pH level, and additional substances [3, 4].

Empirical findings and theoretical frameworks on nanofluid thermal conductivity have been thoroughly reviewed [5, 6]. Applications of nanofluids as cooling agents for heat transfer have been explored [7, 8-10]. The investigation of alumina–water and titania–water nanofluids in turbulent convective heat exchange within pipes had been examined [11]. A proposal on a thermal-transfer correlation for nanofluids to account for energy movement via particle scattering was explored [12]. [13] examined laminar nanofluid convective heat exchange and noted significant improvements in the inlet zone. [14, 15] evaluated the effects of alumina and copper oxide nanofluids on laminar heat transfer in a cylindrical conduit under constant wall temperature conditions. They reported an increase in the heat-transfer coefficient for both nanofluids due to rising nanoparticle concentrations and Peclet number, with alumina showing a greater improvement for copper oxide.

Accordingly, [16] proposed that decreasing viscosity within the boundary layer, with a narrowing of the laminar sublayer, significantly increases the convective heat-transfer coefficient in the turbulent flow regime. Meanwhile, [17] evaluated nanofluids' convective heat transfer and friction coefficient in rectangular microchannels. They used nanofluids containing 170-nm aluminum oxide particles with various particle volume fractions. At a volume fraction of 1.8%, they recorded a 320% increase in convective heat transfer in the laminar regime compared to purified water, without significant frictional losses. They also found that the Nusselt number increases with rising Reynolds number in the laminar flow regime, contradicting traditional thermal Poiseuille-flow analytical findings. Similarly, [18] experimentally investigated laminar convective heat transfer and viscous pressure drop for alumina–water and zirconia–water nanofluids in a flow circuit with a vertically heated pipe. Their measured heat-transfer coefficient and pressure drop aligned well with conventional model predictions for laminar flow; in other words, no unusual heat-transfer enhancement or pressure drop was detected within the measurement uncertainty.

Additionally, [19] introduced new correlations for convective heat transfer and friction coefficients, derived from experiments with various nanofluids under fully developed turbulent flow conditions. Also, [20] studied the effect of cylindrical particles on heat transfer in a microchannel by solving the lattice-Boltzmann equation for fluid motion, coupled with the thermal transport and particle dynamics equations, to directly simulate suspended particle movement. They determined that each particle enhances local heat transfer, improving overall heat-transfer performance. Furthermore, [21] experimentally examined the convective heat transfer of non-Newtonian nanofluids through a uniformly heated cylindrical conduit under turbulent flow conditions, confirming the heat-transfer enhancement of such nanofluids.

Based on numerical fluid dynamics (NFD) calculations, [22] found that the two-phase model provides more accurate nanofluid convective heat transfer predictions than the single-phase framework. In addition, [23] numerically investigated the convective heat transfer of nanofluids in horizontal conduits using a single-phase framework, a two-phase mixture model, and the two-phase Eulerian framework. Their results, validated against experimental measurements indicated that the two-phase mixture model was more accurate. Analogously, [24] numerically examined the impact of nanoparticle motion on fluid flow structure and convective heat transfer in a circular conduit. They concluded that the uneven distribution of nanoparticles resulted in an increased heat-transfer coefficient, while surface friction was reduced.

Nevertheless, [25] analyzed the flow of alumina–water ($Al_2O_3 - H_2O$) nanofluids in two-dimensional rectangular micro conduits to assess heat-transfer enhancement from incorporating nanoparticles into the base fluid, particularly at low Reynolds numbers. They determined that, for a given Reynolds number, the primary enhancement in the Nusselt number was less attributable to higher nanoparticle concentration and more to an increase in fluid velocity required to achieve the specified Reynolds number. Consequently, fixed Reynolds number analyses of nanofluid flow may be inadequate for evaluating heat-transfer properties. Thus, [26] focused on variations in experimental results concerning the effective heat transfer of nanoparticles of different sizes. The initial particle arrangement and any heterogeneous clustering were identified as primary factors influencing effective heat-transfer outcomes for variably sized particles in nanofluids.

However, [27] investigated various particle interactions leading to the aggregation of electrically charged nanoparticles, while [28] developed a model to predict nanoparticle clustering and sedimentation. Focusing on non-spherical nanoparticles, [29] employed Monte Carlo simulations and identified a positive effect of clustering on effective heat transfer. For microchannel heat-dissipation applications, [30] analyzed entropy generation in pure water (H_2O) and copper oxide–water ($CuO - H_2O$) Nanofluid flow within trapezoidal microchannels. Similarly, [31] examined entropy generation in nanofluids due to fluid friction and heat transfer for alumina–water ($Al_2O_3 - H_2O$) Nanofluids in conduits of three different widths. Departing from the assumption that a nanofluid behaves as a homogeneous mixture, [32] proposed two-phase Eulerian–Eulerian simulations to estimate potential heat transfer enhancement in microchannel fluid flow.

Equally, [33] presented a mathematical approach to solve the steady two-dimensional magnetohydrodynamic flow of a viscous, incompressible, electrically conductive fluid past a semi-infinite, moving, porous surface within a permeable medium, using the Homotopy Analysis Method (HAM). In addition, [34] reviewed nanotechnology applications in ground heat exchanger pipes and provided insights for future research on using nanotechnology to reduce costs associated with ground heat exchangers (GHE) for ground source heat pump (GSHP) optimization. Also, [35] investigated nanofluid double-diffusive natural convection within a porous enclosure subjected to various force fields, employing the lattice Boltzmann method (LBM). They found that the effect of the tilt angle is linked to the Darcy number (Da); when Da is low, increasing the tilt angle has no significant impact on heat and mass transport or the flow field.

In their well-published work, [36] investigated planar magnetohydrodynamic boundary-layer nanofluid flow driven by a stretching surface under the influence of suction, using the discrete volume technique (DVT). They noted that the stretching parameter enhances the velocity of the nanofluid. Meaningfully, [37] employed an efficient bvp4c method to review solar energy applications in heat exchangers, focusing on the thermophysical properties of composite nanoparticles. Their findings showed that the concentration profile increases with a higher activation energy parameter.

Reddy [38] conducted a computational analysis of the effects of thermal radiation and chemical reaction on transient magnetohydrodynamic natural convection flow with quadratic initial motion past an infinite, uniform-temperature, vertical, permeable surface, accounting for viscous dissipation. He solved the nondimensional governing equations numerically using the Ritz finite element method. The results indicated a decrease in temperature and velocity within the boundary layer as the radiation parameter increased.

The velocity also increased with higher thermal and solute Grashof numbers but decreased with an increase in the magnetic field parameter. Furthermore, concentration and velocity decreased with increasing Schmidt number and chemical reaction parameter. Likewise, [39] provided an overview of advancements in nanofluids within heat transfer systems, categorizing research into three main flow regimes: laminar, transitional, and turbulent nanofluid flow patterns. They highlighted that, in

heat exchanger design, the superior thermal efficiency of nanofluids enables the creation of more compact and lightweight systems. They also noted that nanoparticles are incorporated into compressor lubricants to improve the performance of refrigeration systems. In specific applications, solid nanoparticles are blended with coolants.

Several researchers [40-43] have emphasized the importance of nonlinear differential equations in scientific and engineering fields, where they are often challenging to solve analytically, prompting exploration of new numerical solutions and integral transformations. Bratu's boundary condition problem, a nonlinear differential equation, is prevalent in applications to solid fuel ignition, thermal combustion, radiative heat exchange, electrospinning for nanofibers, the Chandrasekhar model for cosmic expansion, chemical reactors, and nanotechnology.

Similarly, the porous media equation appears in fluid flow, heat and mass transfer, diffusion, boundary-layer concepts, viscous liquids, and biological systems. Integral transformations, widely used in engineering, applied mathematics, and theoretical physics, simplify both linear and nonlinear differential equations by converting them to an alternative domain, especially when exact solutions are elusive. These transforms, often combined with other methods, are vital for addressing complex boundary value problems in mathematical physics, including thermal exchange, superfluidity, nonlinear diffusion, shock-wave propagation, microscopy, seismology, and radio astronomy. Cuha and Peker [44] highlighted that integral transformations, such as the Kashuri Fundo transform, provide a powerful and reliable approach to solving equations across disciplines such as physics, biochemistry, economics, and engineering by simplifying differential operators in a transformed domain.

However, the incorporation of a theoretical foundation highlights the significance of nonlinear differential equations, such as the porous media equation, which are directly relevant to modeling fluid flow and heat transfer in microfluidic systems. Specifically, the applications of the porous media equation in fluid flow, heat and mass transfer, and viscous liquids align with the present article's focus on thermal transfer and flow modulation. Additionally, the discussion of integral transformations, such as the Kashuri Fundo transform, can support the current article's methodology by justifying their use in simplifying complex boundary value problems encountered in microfluidic heat transfer systems. The areas of applications, such as thermal exchange and nanotechnology, further complement the present research exploration of flexible microfluidic systems, enhancing the context for analyzing nonlinear shear effects and thermal efficiency.

The overview of the present study highlights the significant role of nonlinear differential equations, such as Bratu's boundary condition problem and the porous media equation, in various scientific and engineering fields, including thermal combustion, fluid flow, heat transfer, and nanotechnology. In these areas, analytical solutions are often difficult, leading to the use of numerical methods and integral transformations such as the Kashuri Fundo transform. These transformations make complex boundary value problems easier to handle across disciplines, including mathematics, physics, engineering, and biochemistry, by converting equations into an alternative form.

This also underscored the importance of the present study on thermal management and shear-dependent flow in microfluidic systems, aligning with the journal's focus on innovative research in mechanical, energy, and materials engineering, as well as mathematics and nanotechnology. This research enhances understanding of flexible microfluidic systems to establish a theoretical basis for modeling fluid flow and heat transfer using nonlinear equations and integral transformations, including thermal efficiency and nonlinear shear effects.

In terms of the relationship between the present work and the journal, the present study aligns well with the scope of the journal, as it presents original research in the fields of Applied Mathematics, Mechanical and Energy Engineering, Materials Engineering, Nanoscience and Nanotechnology, all of which

are priority areas for the journal. The current study examines advanced thermal management techniques in microfluidic systems, with a focus on enhancing heat transfer efficiency and elucidating complex shear-dependent flow behaviors, which are crucial for designing modern, energy-efficient devices. By enhancing scientific knowledge and technological development of flexible microfluidic systems, the study supports the journal's publication of high-quality, English-language research that advances understanding across the natural sciences, engineering, and technology.

The present study introduces a novel approach by integrating flow orientation, wall flexibility, and nonlinear shear dilution/enhancement effects into a comprehensive mathematical model for microfluidic heat transfer systems. The transformation of governing partial differential equations (PDEs) into coupled ordinary differential equations (ODEs) using similarity variables, combined with the application of the fourth-order Runge-Kutta-Fehlberg (RKF) method and shooting technique, provides a computationally efficient and accurate approach to analyzing complex thermal and flow dynamics. The consideration of flexible microchannel walls and their impact on nonlinear shear effects represents a unique contribution, as prior studies often assumed rigid boundaries or linear flow behaviors, overlooking these critical interactions.

This work is significant because it enhances the understanding of how flow orientation and channel flexibility influence thermal performance in microfluidic systems, particularly under nonlinear shear conditions. By quantifying the interplay among these factors and their effect on heat transfer efficiency, the study provides a framework for optimizing microfluidic designs. The incorporation of Robin boundary conditions further enhances the model's realism, capturing practical scenarios in microscale heat transfer applications. These findings bridge theoretical modeling and practical implementation, offering actionable insights for improving thermal management in high-precision technologies.

As existing studies on microfluidic heat transfer systems often focus on rigid channels or simplified flow models, the combined effects of wall flexibility, nonlinear shear dilution/enhancement, and flow orientation under realistic boundary conditions, such as Robin boundaries, are neglected. This study addresses this gap by developing a model that accounts for these complex interactions and employs advanced numerical techniques, including the RKF and shooting techniques, to solve the resulting ODEs. By exploring how flexibility and shear effects modulate heat transfer, the research fills a critical gap in understanding and optimizing microfluidic systems for enhanced thermal performance. The applications of this study include, but are not limited to the following areas:

- **Microelectronics Cooling**: The optimized heat transfer model can be applied to design efficient cooling systems for microchips and electronic devices, where precise thermal management is crucial for preventing overheating.
- **Lab-on-Chip Devices**: The findings can enhance the design of microfluidic lab-on-a-chip systems for biomedicalapplications, improving temperature control in chemical reactions and biological assays.
- **Microscale Energy Systems**: The study's insights can inform the development of micro-heat exchangers for energy harvesting or storage devices, enhancing efficiency in compact systems.
- **Pharmaceutical Processing**: The model can be used to optimize microfluidic reactors for drug synthesis, ensuring consistent reaction outcomes through precise thermal regulation.
- **Wearable Medical Devices**: The research can guide the design of microfluidic-based wearable sensors or drug delivery systems, where flexibility and efficient heat dissipation are essential for user comfort and device performance.

Classification of Heat Exchangers

Based on their shapes, heat exchangers (HEs) are classified into three types:

Indirect Contact HEs: This device facilitates efficient heat transfer between two fluids without direct mixing, using a solid barrier to prevent particle exchange. Plate heat exchangers, for example, are widely used in industrial processes such as refrigeration and chemical processing, ensuring effective temperature control and preventing cross-contamination. Indirect-contact heat exchangers offer versatility in handling diverse fluids with varying properties, providing high thermal efficiency and reliability while reducing the risk of corrosion and fouling. Their design makes them ideal for applications where maintaining fluid purity is essential for effective heat transfer. It is shown in Figure 1.

Double-Pipe HEs: A double-pipe heat exchanger, shown in Figure 2, consists of two concentric pipes designed for efficient heat transfer, accommodating fluids in either counter-flow or parallel-flow configurations. Its compact design makes it ideal for space-constrained environments, facilitating easy installation, maintenance, and cleaning. With the ability to handle fluids of varying properties, it offers a cost-effective solution for moderate heat transfer needs in industries such as chemical processing and HVAC (heat, ventilation, and air conditioning) systems. Despite its simplicity, the double-pipe heat exchanger efficiently transfers heat between fluid streams, making it a reliable choice for various industrial applications.

Shell-and-Tube HEs: These are widely recognized for their versatility and efficiency in heat transfer between two fluids, featuring multiple tubes within a cylindrical shell to maximize surface area contact.

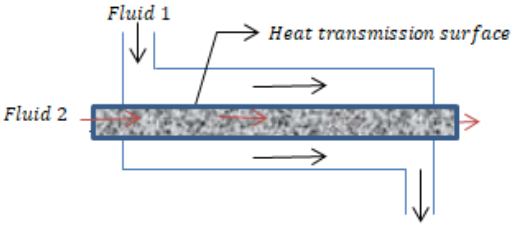

Figure 1. Indirect contact type heat exchanger

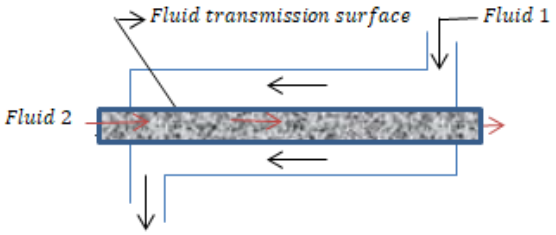

Figure 2. Double pipe heat exchanger

They excel in high-pressure and high-temperature environments, serving industries such as chemical processing, manufacturing, and power generation. Offering flexibility with parallel-flow and counter-flow configurations, they handle a variety of fluids with ease and facilitate straightforward maintenance and cleaning. Known for their durability and scalability, they are a preferred choice for industrial applications requiring efficient heat transfer. It is represented in Figure 3.

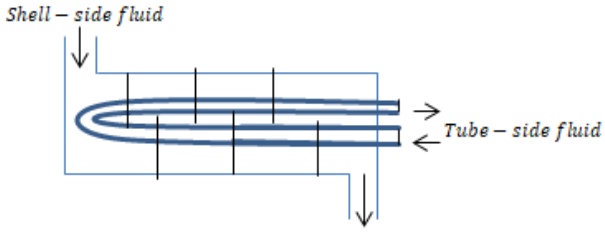

Figure 3. Shell–and–-tube type heat exchanger

2. Mathematical Formulation of the Problem

A steady, two-dimensional, laminar, free convective boundary-layer flow of a viscous, incompressible, electrically conducting fluid along a vertical, exponentially stretching plate with bi-dilatant or shear-thinning properties is analyzed. Meanwhile, the plate remains flexible. Due to the stretching nature of the plate, buoyancy effects, driven by variations in the temperature distribution of suspended nanoparticles and temperature-dependent viscosity, induce motion in the incompressible, non-Newtonian fluid. This results in the plate's elongation along the x-axis, with the origin fixed at $x = y = 0$.

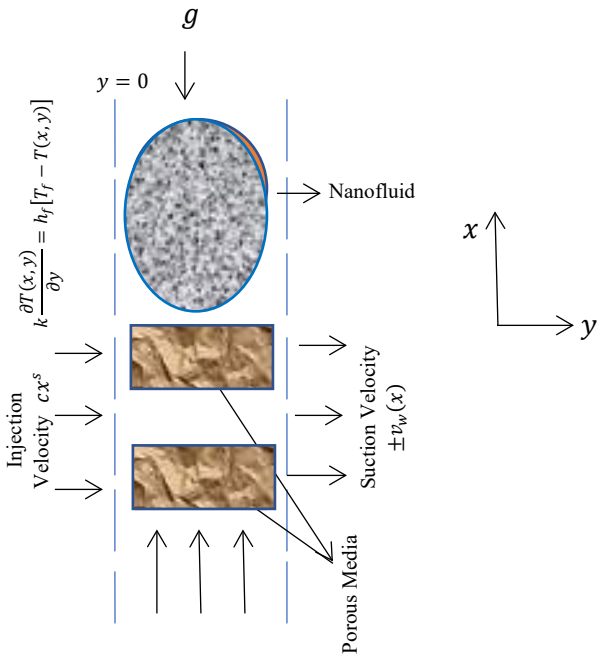

Figure 4. Flow model and coordinate system

The flow configuration is illustrated in Figure 4. A uniform magnetic field of strength B_0 is applied perpendicular to the flow direction, and the pressure remains constant along the wall. Comparison of the induced and applied magnetic fields reveals that the former is negligible due to its significantly smaller magnitude. Based on the approximation of [45], the governing boundary-layer equations are expressed as follows:

Continuity equation

$$\frac{\partial u}{\partial x}+\frac{\partial v}{\partial y}=0 \tag{1}$$

Momentum equation

$$u\frac{\partial u}{\partial x}+v\frac{\partial u}{\partial y}=\frac{\mu_{ff}}{\rho_{ff}}\left[\frac{\partial^2 u}{\partial y^2}+g_a(\rho\beta)_{ff}(T-T_\infty)cos\gamma-\frac{\sigma B_0^2}{\rho}(u-u_\infty)-\frac{v_f}{k}u\right] \tag{2}$$

Energy conservation equation

$$u\frac{\partial T}{\partial x}+v\frac{\partial T}{\partial y}=\alpha_{ff}\frac{\partial^2 T}{\partial y^2}-\frac{k}{(\rho C_p)_{ff}}\frac{\partial q_r}{\partial y}+\frac{(\rho C)_{ff}}{Q_0(T-T_\infty)}+\frac{1}{(\rho C)_{ff}}h''' \tag{3}$$

Mass Conservation equation

$$u\frac{\partial C}{\partial x}+v\frac{\partial C}{\partial y}=M_D\frac{\partial^2 C}{\partial y^2}+\frac{kv_f}{T_\infty}\frac{\partial T}{\partial y}\frac{\partial C}{\partial y}-C^*\left(\frac{\partial C}{\partial y}\right)^n \tag{4}$$

Subject to the following boundary conditions.

$$\begin{aligned}&\text{at } y=0\text{: } u(x,y)=u=cx^s, C=C_w,\\ &v(x,y)=\pm v_w(x),\\ &k\frac{\partial T(x,y)}{\partial y}=h_f\left[T_f-T(x,y)\right].\\ &\text{as } y\to\infty\text{: } u\to 0, v\to 0, T\to T_w, C\to C_\infty\end{aligned} \tag{5}$$

The coordinates are $x$and y, while the velocity components are represented as u and v. The terms, μ_{ff} and α_{ff} implies absolute and kinematic viscosity, $g_a=$ acceleration owing to gravity, $\rho=$ base fluid density, $\beta=$ heat enlargement quantity of the base liquid, $B_0=$ magnetic field strength, $\gamma=$ inclination angle, $\sigma=$ electrical conductivity, $k=$ porosity factor, $C_p=$ Specific heat capacity at a fixed pressure, $q_r=$ thermal radiative fluidity, $Q_0=$ heat source term, $M_d=$coefficient of Brownian movement, $C^*=$ chemical reactivity coefficient, $n=$ diluting/enhancing shear term, T and C are ambient temperature and concentration, T_∞ and C_∞ refers to temperature and concentration far from the wall, $R_{a_x}=\frac{g_a(\rho\beta)_{ff}(T-T_\infty)}{v_{\alpha_{ff}}}$, refers to the Rayleigh factor, $h'''=\frac{xR_{a_x}^{\frac{1}{2}}}{2x^2}[A(T_s-T_\infty)f'(\eta)+\theta(T-T_\infty)]$ is the thermal dependent variable source and $A>0$ corresponds to internal heat generation [46].

2.1. Similarity transformation variable

The similarity variables needed to transform equations (1) – (4) are:

$$\begin{aligned}&\eta=y\sqrt{\frac{u_0}{2lv_{ff}}}\;e^{\frac{Nx}{2l}}, u=u_0(x)e^{\frac{Nx}{2l}}f'(\eta)\\ &c=c_0e^{\frac{Nx}{2l}}\emptyset(\eta), \theta(\eta)=\frac{T-T_\infty}{T_s-T_\infty},\\ &\emptyset(\eta)=\frac{C-C_\infty}{C_s-C_\infty}, \psi=\alpha_s Ra_x^{\frac{1}{4}}f(\eta),\\ &v=-N\sqrt{\frac{v_{ff}u_0}{2l}}\;e^{\frac{Nx}{2l}}[f(\eta)+\eta f'(\eta)]\\ &u=\frac{\partial\psi}{\partial y},\; v=-\frac{\partial\psi}{\partial x}\end{aligned} \tag{6}$$

3. Method of Solution

The fourth-order Runge-Kutta (RK4) method is a numerical technique for solving coupled ordinary differential equations (ODEs), valued

for its accuracy and stability. When applied to a system of coupled ODEs, RK4 approximates the solution by discretizing the independent variable (e.g., time or space) and iteratively computing the dependent variables at each step. For each ODE in the system, RK4 evaluates the derivatives at four intermediate points within a step, combining them to achieve a fourth-order accurate approximation of the solution. This method is particularly effective for nonlinear systems, as it handles coupling by simultaneously updating all variables at each step. Its robustness makes it suitable for microfluidic heat transfer problems, where coupled ODEs arise from transforming partial differential equations governing flow and thermal fields.

Similarly, the Runge-Kutta-Fehlberg (RKF) method enhances RK4 by incorporating adaptive step-size control, improving computational efficiency for coupled ODEs. It employs a pair of Runge-Kutta methods (typically fourth- and fifth-order) to estimate the local truncation error, dynamically adjusting the step size to maintain accuracy. The shooting method complements these techniques when solving boundary value problems (BVPs) for coupled ODEs, such as those with Robin boundary conditions. It converts the BVP into an initial value problem by guessing initial conditions, solving the system using RKF, and iteratively adjusting the guesses (e.g., via Newton's method) until the boundary conditions are satisfied. In microfluidic systems, the shooting method is critical for handling nonlinearities and coupled effects, ensuring accurate solutions for variables such as temperature and velocity under complex flow orientations and shear effects.

The bvp4c solver function in Maple 16 is employed to address the problem under consideration. It uses collocation techniques, iteratively refining the solution space to match the boundary conditions, offering a reliable and efficient means to approximate solutions. The solver uses the residual of the continuous solution to control errors and select an appropriate mesh, dividing the integration interval into smaller subintervals.

The solver then addresses a system of algebraic equations generated by integrating collocation requirements and boundary constraints across these subintervals. If the computed solution fails to meet the specified tolerance conditions for each subinterval, the solver iteratively adjusts the mesh. These techniques are used to analyze phenomena such as heat transfer in fin arrays and flow stability. Together, these methods provide a powerful framework for solving coupled ODEs with high precision and efficiency. The stream function $\psi(x,y)$ defined as $u = \frac{\partial \psi}{\partial y}$ and $v = -\frac{\partial \psi}{\partial x}$ identically satisfies equation (1). In line with the approximation of the Roseland expression for radiative effect, we have

$$q_r = -\left(\frac{4\sigma^*}{3k_0}\right)\frac{\partial T'^4}{\partial y} \tag{7}$$

Such that the mean absorption factor k_0 and Stefan-value $\sigma \approx 1.3806 \times 10^{-23}$. By expressing T^4 about T_∞, Taylor's series expansion yields

$$T^4 \cong T_\infty^4 + 3T_\infty^3(T - T_\infty) + 6T_\infty^2(T - T_\infty)^2 + \cdots \tag{8}$$

By neglecting the terms of greater degrees in equation (8), we obtain

$$T^4 \cong 4TT_\infty^3 + 3T_\infty^4 \tag{9}$$

Thus, using equations (7) and (9) in equation (3) streamlines to

$$u\frac{\partial T}{\partial x} + v\frac{\partial T}{\partial y} = \alpha_{ff}\frac{\partial^2 T}{\partial y^2} - \frac{k}{(\rho C_p)_{ff}}\frac{16\sigma^* T_\infty^3}{3k_0} + \frac{Q_0(T-T_\infty)}{(\rho C)_{ff}} + \frac{1}{(\rho C)_{ff}}h''' \tag{10}$$

Plugging equation (6) into equations (2), (4), and (10), respectively, gives,

$$\frac{d^3 f}{d\eta^3} - \frac{1}{2}Nf(\eta)\frac{d^2 f}{d\eta^2} + Nf(\eta)\frac{d^2 f}{d\eta^2} - (M+P)\frac{df}{d\eta} + Gr\theta(\eta)\cos(\gamma) = 0 \tag{11}$$

$$\frac{d^2\theta}{d\eta^2}\left(1 + \frac{4}{3}S\right) + Prf(\eta)\frac{d\theta}{d\eta} + \Delta_H\frac{d\theta}{d\eta} + NA\frac{df}{d\eta} + Ec\left(\frac{df}{d\eta}\right)^2 = 0 \tag{12}$$

$$\frac{d^2\phi}{d\eta^2} + ScNf(\eta)\frac{d\phi}{d\eta} + \frac{N}{Nt}\frac{d\theta}{d\eta}\frac{d\phi}{d\eta} - R_c\left[\frac{d\phi}{d\eta}\right]^n = 0 \quad (13)$$

The transformed boundary conditions are stated as:

$$f(\eta) = 0,\ f'(\eta) = 1,\ \theta'(\eta) = -R_o\big(1-\theta(\eta)\big),\ \phi(\eta) = 1 \quad \text{at } \eta = 0 \quad (14)$$

$$f'(\eta) = 0,\ \theta(\eta) = 0,\ \phi(\eta) = 0 \text{ as } \eta \to \infty \quad (15)$$

such that the following parameters,

$$N = \frac{kU_0}{\nu Ra_x^{\frac{1}{2}}}e^{\frac{Nx}{l}},\quad M = \frac{2L\sigma B_0^2}{\rho_{ff}U_0},\quad Pr = \frac{\upsilon_{ff}}{\alpha_{ff}},\quad Gr = \frac{2Lg\beta_{ff}T_0}{U_0^2},\ Ec = \frac{U_0^2}{T_0(c_p)_{ff}},\ \Delta_H = \frac{2LQ^*}{(\rho c_p)_{ff}U_0},\ Sc = \frac{\upsilon_{ff}}{M_D},\ P = \frac{2L\rho}{kU_0},\ \gamma, A, Nt = \frac{U_0T_0C_0(k\nu)^2}{2M_d\sqrt{\frac{U_0}{2\nu l}}e^{-\frac{Nx}{l}}},\ R_c = \frac{R_cC_0}{M_d},\ R_o,$$

n, implies stretching, magnetic intensity, Prandtl, radiation, improved thermal Grashof, Eckert, volumetric heat source, mass diffusion, flexibility, flow orientation, and thermally dependent characteristics, Thermophoresis, kinetic, Robin boundary condition, and non-linear shear-thinning/thickening parameters.

3.1. Numerical procedure

To apply the methods described above to equations (11) – (13) and (14) – (15), the boundary value problems (BVPs) were converted into initial value problems (IVPs) by transforming higher-order ordinary differential equations (ODEs) into a system of first-order ODEs. The Newton-Raphson method was used to locate roots. Subsequently, the fourth-order Runge-Kutta-Fehlberg (RKF) method was employed to solve the IVPs. The shooting method was implemented using Maple V. 16. The system of first-order ODEs is expressed as follows:

$$f = y_1,\ f' = y_2,\ f'' = y_3,\ f''' = y_3' \quad (16)$$

$$y_3' = \frac{1}{2}Ny_1y_3 - Ny_1y_3 + (M+P)y_2 - Gry_4\cos(\gamma) \quad (17)$$

$$y_4 = \theta,\ y_5 = \theta',\ \theta'' = y_5' \quad (18)$$

$$y_5' = -\frac{1}{\left(1+\frac{4}{3}S\right)}[Pry_1y_5 + \Delta_H y_5 + NAy_2 + Ec(y_2)^2] \quad (19)$$

$$y_6 = \phi,\ y_7 = \phi',\ \phi'' = y_7' \quad (20)$$

$$y_7' = -ScNy_1y_7 - \frac{N}{Nr}y_5y_7 + R_c(y_7)^n \quad (21)$$

The corresponding wall conditions include,

$$y_1(\eta) = 0,\quad y_2(\eta) = 1,\quad y_5(\eta) = -R_o\big(1 - y_4(\eta)\big),\ y_6(\eta) = 1 \quad \text{at } \eta = 0 \quad (22)$$

$$y_2(\eta) = 0,\ y_4(\eta) = 0,\ y_6(\eta) = 0 \quad \text{as} \quad \eta \to \infty \quad (23)$$

The quantities of the rates of heat and mass transfer are determined by computing the local Nusselt number Nu_x and Sherwood number Sh_x, respectively.

$$Nu_x = \frac{xq_w}{T_w - T_\infty} = -\sqrt{\frac{xRe_x}{2L}}\theta'(0) \quad (24)$$

$$Sh_x = \frac{xj_w}{C_w - C_\infty} = -\sqrt{\frac{xRe_x}{2L}}\phi'(0) \quad (25)$$

4. Results and Discussion

Numerical results for various fluid parameters were obtained using the computational method described earlier. Figures 5 – 31 present the graphical representations, including legends. Figure 5 illustrates the impact of shear-thinning and shear-thickening behavior (characterized by the flow behavior index, n) on species concentration. It demonstrates how a fluid's viscosity responds to applied shear stress. Shear-thinning fluids, such as ketchup, exhibit a decreased viscosity with increasing shear rates, facilitating easier flow under higher shear stress.

Conversely, shear-thickening fluids, such as a cornstarch-water mixture, exhibit increased viscosity with higher shear rates, leading to greater resistance to flow. According to [47], these behaviors are described by the flow behavior index in the Herschel–Bulkley model: n < 1 for shear-thinning fluids and greater than 1 for shear-thickening fluids. An increase in the

shear-thickening parameter leads to higher viscosity under shear, which impedes mixing and (n) leads to higher viscosity under shear, which hinders mixing and may result in localized regions of higher species concentration due to reduced diffusion.

Applying a magnetic field to an electrically conductive fluid, such as plasma or liquid metal, generates a resistive force known as the Lorentz force. This force opposes the fluid's motion, reducing its velocity, as shown in Figure 6. As fluid motion slows due to the Lorentz force, convective heat and mass transport diminish, leading to an accumulation of thermal energy and species concentration within the fluid, as shown in Figures 7 and 8.

Several studies have shown that increasing the magnetic field parameter reduces fluid velocity while elevating temperature and concentration profiles due to suppressed convective transport. In air coils, the magnetic field modulates the fluid motion in Magnetohydrodynamic (MHD)-enhanced designs improve heat transfer efficiency in liquid metal systems.

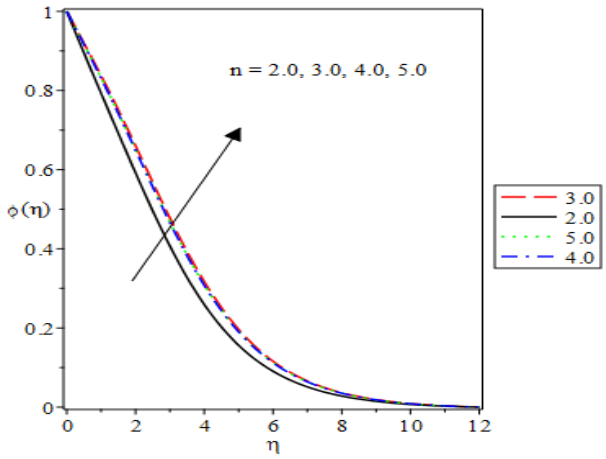

Figure 5. Effect of n on $\phi(\eta)$

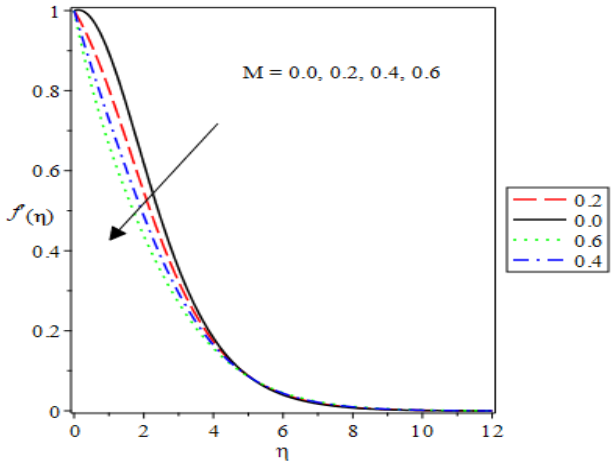

Figure 6. Effect of M on $f'(\eta)$

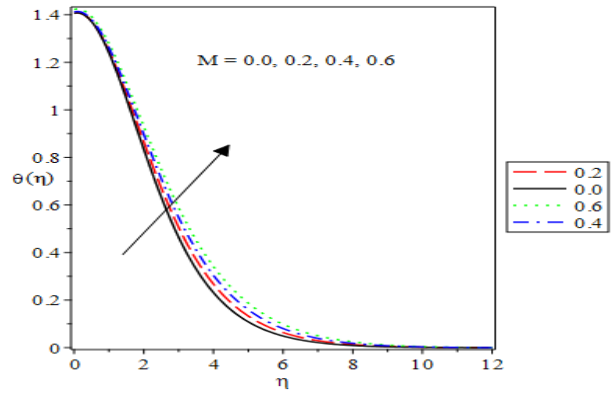

Figure 7. Effect of M on $\theta(\eta)$

It influences liquid metal coolant behavior in nuclear reactors [48] and governs convective heat transfer in MHD flows, refining energy transport models in thermal science [49]. Its role in enhancing plasma control in MHD generators increases efficiency in solar power systems [50]. In nanotechnology, magnetic fields enhance

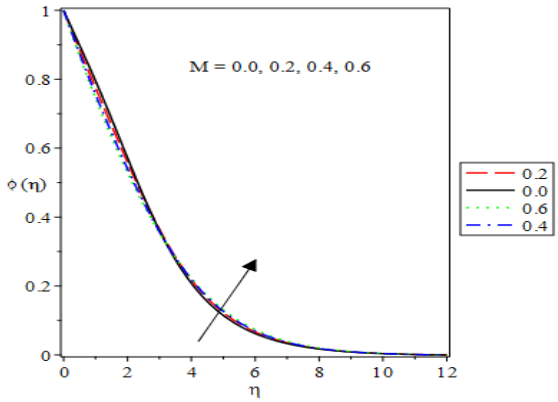

Figure 8. Effect of M on $\phi(\eta)$

nanofluid dynamics, improving thermal conductivity.In manufacturing, they control molten metal flows during casting, enhancing product quality. In biomedical engineering,

magnetic fields affect blood flow (a weakly conducting fluid) in applications such as magnetic resonance imaging (MRI) and magnetic therapies. Thus, the magnetic field parameter significantly shapes fluid and thermal dynamics, driving innovation across these domains.

The effects of increasing the flexibility parameter (P) on velocity, temperature, and concentration distributions are shown in Figures 9, 10, and 11, respectively. This parameter, often associated with viscoelastic fluids, quantifies the fluid's resistance to deformation and its tendency to return to its original state. An increase in P indicates a longer fluid relaxation time, enhancing the fluid's elastic properties. This heightened flexibility introduces additional resistance to flow, reducing fluid velocity. The decreased velocity weakens convective heat and mass transfer, leading to an accumulation of thermal energy and species concentration within the fluid.

Consequently, both temperature and concentration profiles increase due to suppressed convective transport. This behavior has been observed in studies examining the effects of flexibility on convective heat and mass transfer in viscoelastic fluid flows. In heat sinks, the flexibility of viscoelastic fluids enhances mixing and heat transfer under shear. In nuclear reactors, it influences the coolant behavior in polymer-additive flows, potentially reducing drag and improving heat removal.

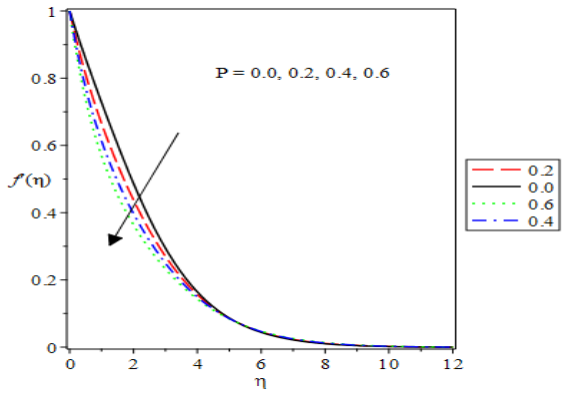

Figure 9. Effect of P on $f'(\eta)$

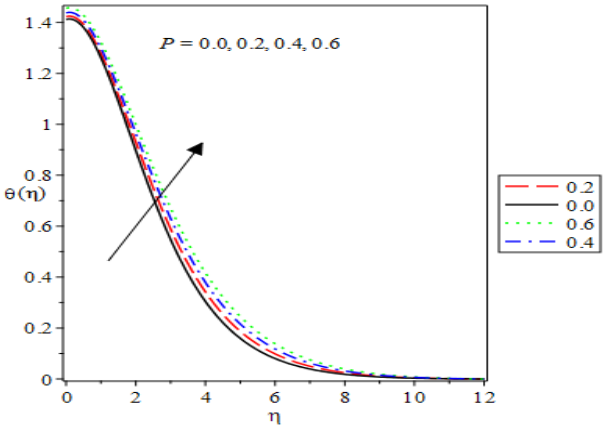

Figure 10. Effect of P on $\theta(\eta)$

In thermal science, flexibility modifies convective heat transfer in non-Newtonian fluids, refining boundary-layer models. In solar power systems, the elastic properties of working fluids may affect flow stability in flexible collectors. In nanotechnology, flexibility influences the dynamics of polymer-based nanofluids, enhancing thermal conductivity. In manufacturing, it governs polymer extrusion and molding, influencing heat transfer and product quality. In biomedical engineering, flexibility affects blood flow (a viscoelastic fluid) and tissue mechanics, altering heat distribution. The flexibility parameter thus bridges rheological and thermal phenomena, optimizing system performance.

The flow orientation parameter, often represented by the inclination angle (γ), significantly affects fluid flow characteristics. As the inclination angle increases, the component of the gravitational force acting along the flow direction decreases, reducing buoyancy-driven flow velocity, as shown in Figure 12. This deceleration weakens convective heat and mass transfer, leading to an accumulation of thermal energy and species concentration near the surface.

Consequently, both temperature and concentration distributions increase, as illustrated in Figures 13 and 14, due to suppressed convective transfer. This parameter, which describes the alignment of fluid flow relative to surfaces or gravitational fields (e.g., horizontal, vertical, or inclined), plays a critical role in convective heat transfer and fluid dynamics across various scientific and engineering domains.

In heat exchangers, flow orientation influences heat transfer efficiency, with vertical orientations typically enhancing natural convection. In nuclear reactors, the flow orientation parameter affects coolant circulation, particularly in vertical fuel channels, where buoyancy enhances heat removal. In thermal science, it governs the interaction between forced and natural convection, refining heat transfer models.

Hence, [51] noted that in solar power systems, the flow orientation influences the airflow in collectors or chimneys, optimizing thermal performance. In nanotechnology, it affects fluid dynamics around nanostructures, impacting heat dissipation. In manufacturing, flow orientation alters heat transfer during material cooling or solidification, impacting product quality. In biomedical engineering, flow orientation influences blood flow in vessels, affecting tissue heat distribution [52].

The effect of the stretching parameter (N) on velocity distribution is shown in Figure 15. It is commonly encountered in fluid dynamics and heat transfer analyses and plays a critical role across multiple scientific and engineering domains by quantifying the deformation or extension of surfaces or fluids under various physical conditions.

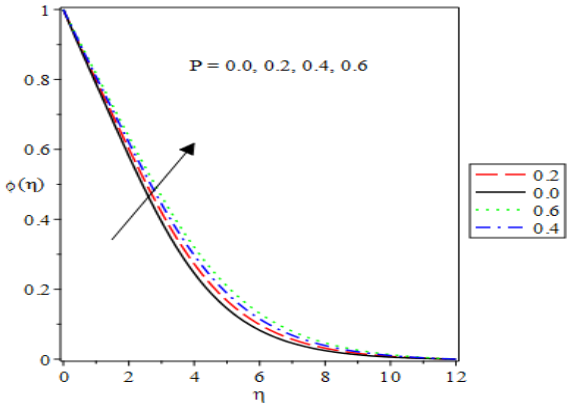

Figure 11. Effect of P on $\phi(\eta)$

Thus, the flow orientation parameter significantly shapes convective efficiency and system design.

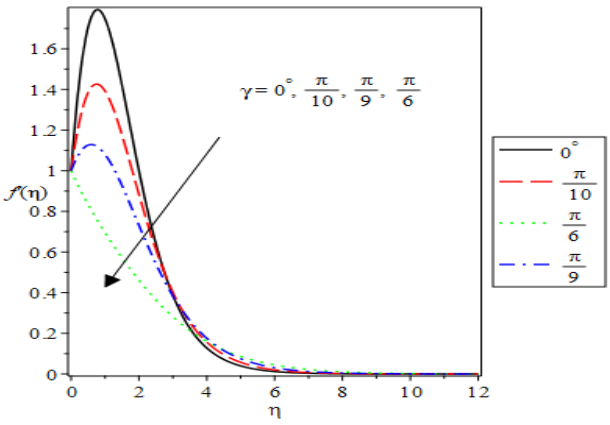

Figure 12. Effect of γ on $f'(\eta)$

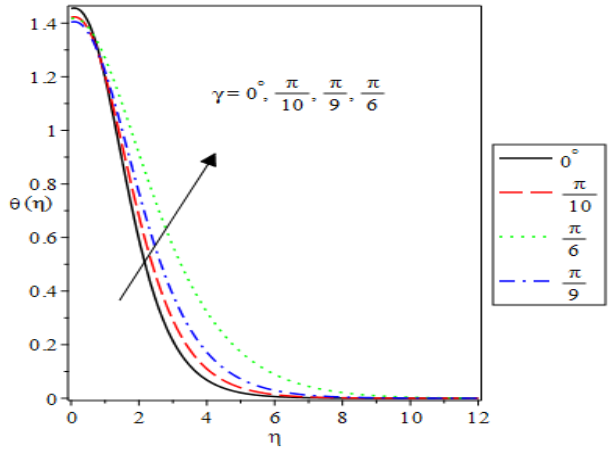

Figure 13. Effect of γ on $\theta(\eta)$

It influences the convective heat transfer rate by altering boundary-layer thickness, enhancing efficiency as stretching surfaces (e.g., in tube or plate designs) promote fluid mixing and heat dissipation in heat exchangers. In breeder reactors, the stretching parameter affects coolant flow behavior over fuel rods, impacting heat removal and safety by modulating thermal gradients and preventing hotspots.

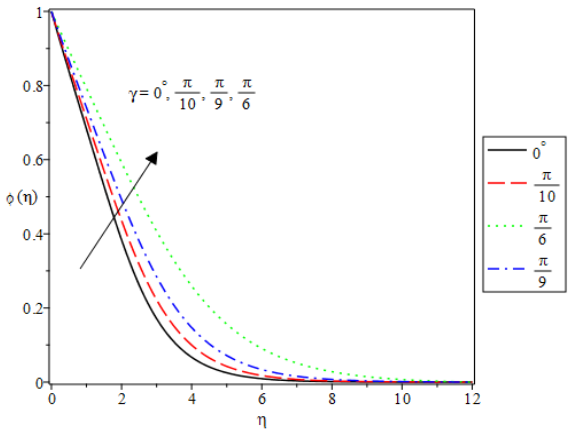

Figure 14. Effect of γ on $\phi(\eta)$

In thermal science, it governs the interaction between stretching surfaces and temperature distributions, enabling precise modeling of heat conduction and convection in complex systems.

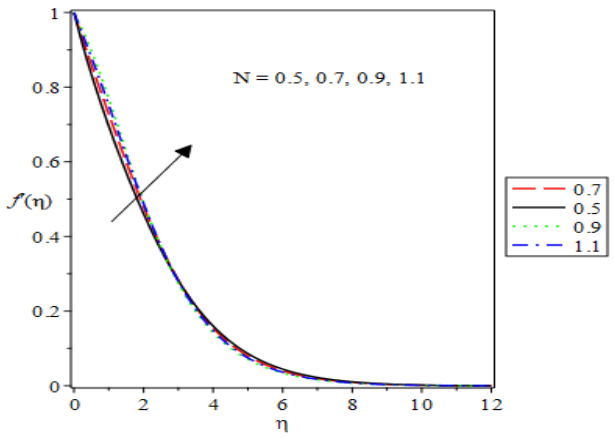

Figure 15. Effect of N on $f'(\eta)$

It is commonly encountered in fluid dynamics and heat transfer analyses and plays a critical role across multiple scientific and engineering domains by quantifying the deformation or extension of surfaces or fluids under various physical conditions. It influences the convective heat transfer rate by altering boundary-layer thickness, enhancing efficiency as stretching surfaces (e.g., in tube or plate designs) promote fluid mixing and heat dissipation in heat exchangers. In breeder reactors, the stretching parameter affects coolant flow behavior over fuel rods, impacting heat removal and safety by modulating thermal gradients and preventing hotspots. In thermal science, it governs the interaction between stretching surfaces and temperature distributions, enabling precise modeling of heat conduction and convection in complex systems.

In nanotechnology, the parameter is crucial for understanding heat transfer in stretched nanostructures, such as graphene sheets or nanotubes, where surface stretching modifies thermal conductivity and energy transport at the nanoscale. Similarly, in biomedical engineering, it influences processes like tissue stretching in bioreactors or blood vessel dynamics, affecting heat and mass transfer rates critical for cell growth, drug delivery, or thermal therapies. Across these fields, the stretching parameter bridges physical deformation and thermal performance, driving advancements in design and functionality.

The Robin parameter (C), representing a linear combination of temperature and its gradient at a surface, quantifies the balance between convective and conductive heat transfer, significantly influencing thermal behavior across various fields. Increasing C enhances the convective heat transfer rate, promoting faster thermal energy dissipation from the surface into the fluid. Consequently, the surface temperature decreases, as shown in Figure 16, due to more effective heat removal. This principle is critical in designing and operating heat exchangers, nuclear reactors, and solar power systems, where optimizing the convective heat transfer coefficient ensures efficient thermal management and prevents overheating. In heat exchangers, the Robin parameter models heat transfer at finned surfaces, where convection and conduction interact, improving design accuracy.

In nuclear reactors, it governs heat flux at fuel rod boundaries for safety analysis. In thermofluidic science, it refines the boundary condition models, enhancing solutions for heat conduction problems.

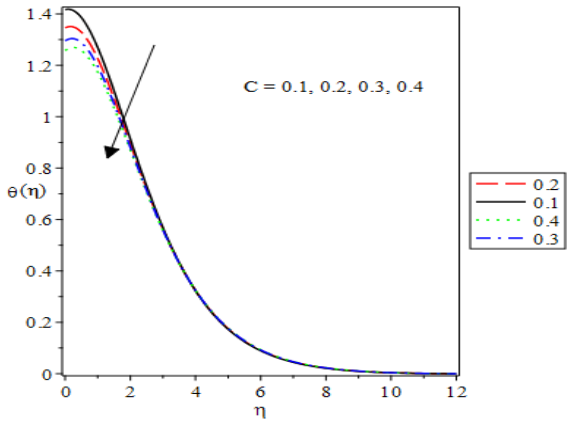

Figure 16. Effect of C on $\theta(\eta)$

In solar power systems, it influences heat loss from absorbers to the environment, optimizing efficiency. In manufacturing, it models heat transfer during the cooling of molded parts, affecting product quality. In biomedical engineering, it simulates heat exchange in tissues during thermal therapies. The Robin parameter thus bridges surface heat transfer mechanisms, driving precision in thermal management.

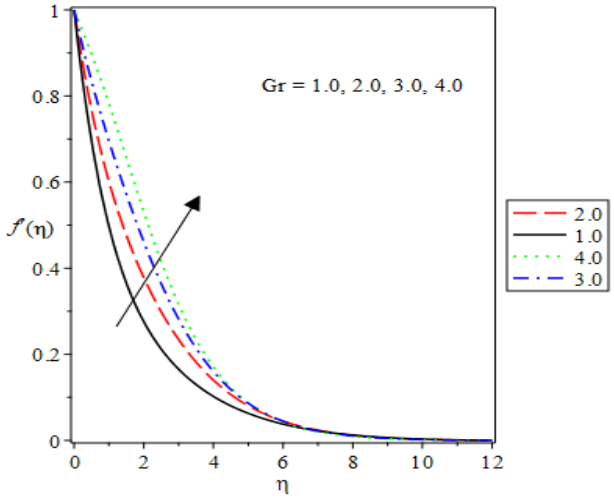

Figure 17. Effect of Gr on $f'(\eta)$

Figure 17 illustrates the impact of the thermal buoyancy (Grashof) number (Gr) on the velocity distribution. This parameter represents the ratio of buoyancy to viscous forces in a fluid. An increase in Gr indicates that buoyancy forces dominate, enhancing natural convection currents and increasing fluid velocity. This relationship has been observed in studies where higher values of the Grashof number (Gr) correspond to elevated velocity profiles due to intensified buoyancy effects. In heat exchangers, Gr governs free convection, enhancing heat transfer in designs reliant on buoyancy-driven flows. It influences the coolant circulation in passive safety systems for the removal of heat without pumps in breeder reactors.

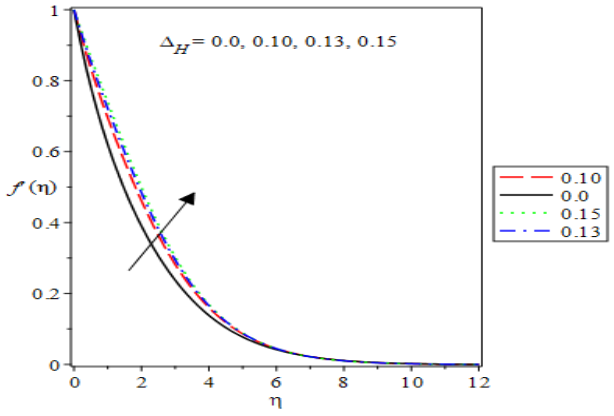

Figure 18. Effect of Δ_H on $f'(\eta)$

In solar power systems, Gr drives airflow in solar chimneys or collectors, optimizing energy capture. In manufacturing, it affects buoyancy-driven flows in molten materials, influencing casting quality. The Grashof number thus underpins natural convection phenomena, guiding system efficiency and design. The volumetric heat source parameter (Δ_H), representing internal heat generation within a fluid, significantly affects its thermal and flow behavior. An increase in Δ_H elevates the fluid's internal energy, raising its temperature (Figure 19) and reducing its density, which enhances buoyancy forces, accelerates fluid motion, and increases velocity (Figure 18). These intensified convective currents promote. species transfer, resulting in a higher concentration level (Figure 20).

This behavior is evident when increased heat source parameters lead to elevated velocity, temperature, and concentration profiles [53]. In air coils, it accounts for internal heat generation (e.g., from chemical reactions), which improves design accuracy. In nuclear reactors, it quantifies heat from fission for core temperature management. In thermal science, it refines models of heat transfer in media with distributed sources. In nanotechnology, it governs thermal effects in nanostructures under localized heating, such as laser exposure. In biomedical engineering, it is applied to hyperthermia treatments, where controlled heat generation in tissues enhances therapeutic outcomes. The volumetric heat source parameter thus bridges heat generation and transfer, driving precision in design and analysis.

The influence of the thermal radiation parameter on velocity, temperature, and species concentration is shown in Figures 21, 22, and 23, respectively. The thermal radiation parameter, a dimensionless quantity representing the relative significance of radiative heat transfer compared to conduction or convection, is critically important across various scientific and engineering disciplines. It accounts for radiative heat transfer within fluid flow. An increase in this parameter enhances radiative heat flux, raising the fluid's temperature and reducing its density, which intensifies buoyancy forces and increases flow velocity. Higher temperatures can reduce fluid viscosity, further contributing to velocity enhancement.

However, the elevated temperature also accelerates species diffusion, decreasing concentration levels within the fluid. In heat

exchangers, the parameter governs the contribution of radiation to overall heat transfer, enhancing efficiency by dominating particularly in high-temperature systems like gas-cooled designs, where radiative effects can overcome convective losses.

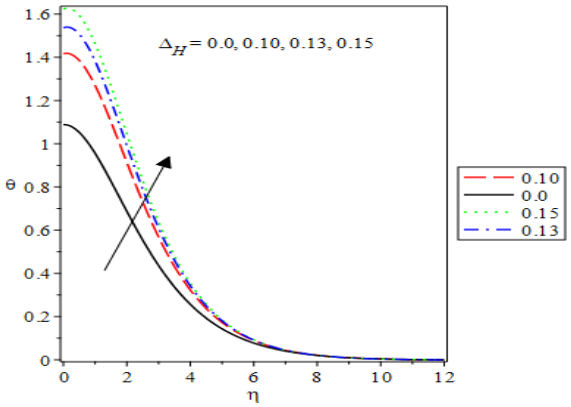

Figure 19. Effect of Δ_H on $\theta(\eta)$

In nuclear reactors, it is essential for modeling heat dissipation from fuel rods and reactor walls, especially under extreme conditions where radiation becomes a primary mode of energy transfer, ensuring structural integrity and safety. In thermal science, it provides a framework for analyzing energy exchange in systems with significant temperature gradients, improving predictions of heat flux for both terrestrial and space applications.

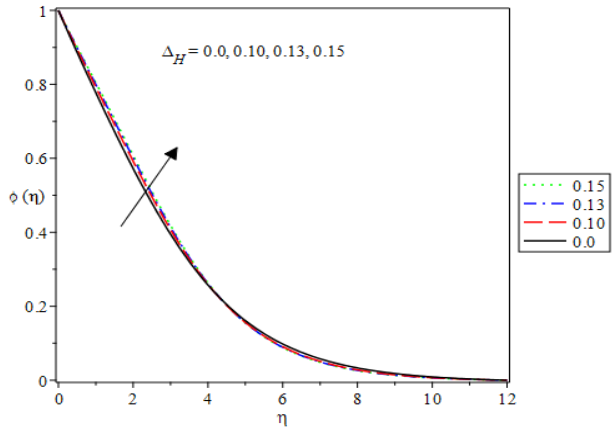

Figure 20. Effect of Δ_H on $\phi(\eta)$

In nanotechnology, the thermal radiation parameter influences the performance of nanoscale devices, such as thermal sensors or energy-harvesting systems, where radiative heat transfer dominates due to high surface-to-volume ratios. In biomedical engineering, it affects applications like laser-based thermal therapies or Hyperthermia treatments require precise control of radiative heat transfer to tissues to ensure effectiveness and patient safety. Therefore, the thermal radiation parameter acts as a key indicator of radiative influence, guiding design and operational strategies in these fields. Variable fluid properties, such as viscosity and thermal conductivity that depend on temperature, significantly impact flow, temperature, and concentration distributions, as shown in Figures 24, 25, and 26. These properties influence system performance across multiple disciplines by adding nonlinearity and complexity to heat and mass transfer processes.

As temperature-dependent properties increase, fluid viscosity decreases with rising temperature, reducing internal resistance and boosting fluid velocity. This higher velocity enhances convective heat transfer, which further raises the fluid's temperature. The increase in temperature then further reduces viscosity, creating a feedback loop that sustains higher velocities and temperatures.

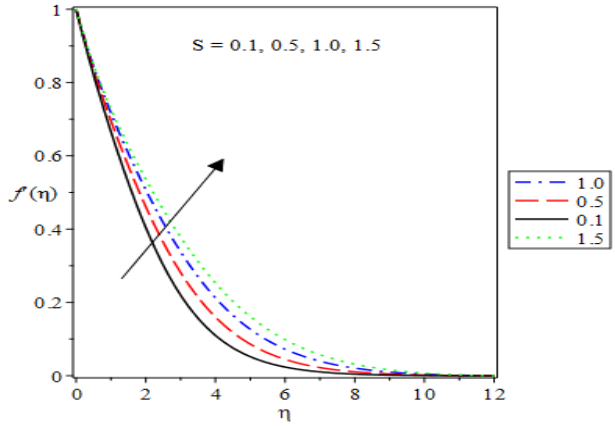

Figure 21. Effect of S on $f'(\eta)$

In heat exchangers, these properties influence fluid flow and heat transfer efficiency, as viscosity decreases with rising temperature, convective currents strengthen, while variations in thermal conductivity alter heat diffusion rates, critical for optimizing exchanger design.

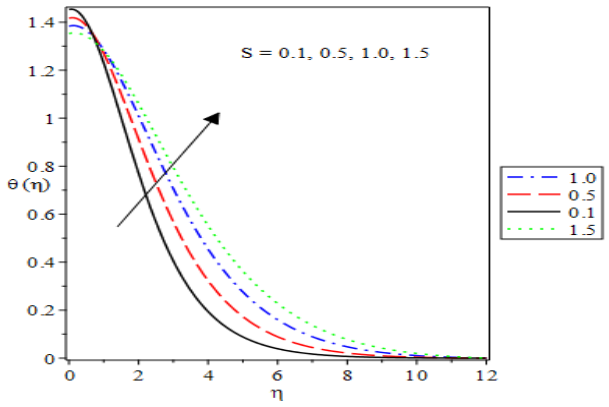

Figure 22. Effect of S on $\theta(\eta)$

In nuclear reactors, temperature-dependent fluid properties influence coolant performance, especially in high-temperature environments, where lower viscosity improves circulation and changing thermal conductivity affects heat removal from fuel assemblies, ensuring operational stability.

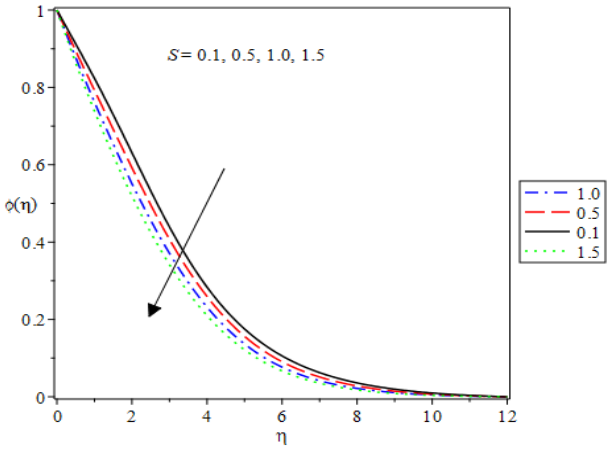

Figure 23. Effect of S on $\phi(\eta)$

In thermal science, the parameter is essential for accurately modeling heat transfer in fluids under varying conditions, enabling precise predictions of thermal boundary layers and energy transport in complex systems. In nanotechnology, variable properties govern thermal management in nanoscale materials, such as nanofluids or thin films, where temperature-induced changes in viscosity and conductivity affect heat dissipation and device reliability. In biomedical engineering, they influence blood flow dynamics and tissue interactions, where temperature-dependent viscosity affects perfusion rates and thermal conductivity variations impact heat distribution during procedures like cryosurgery or thermal ablation.

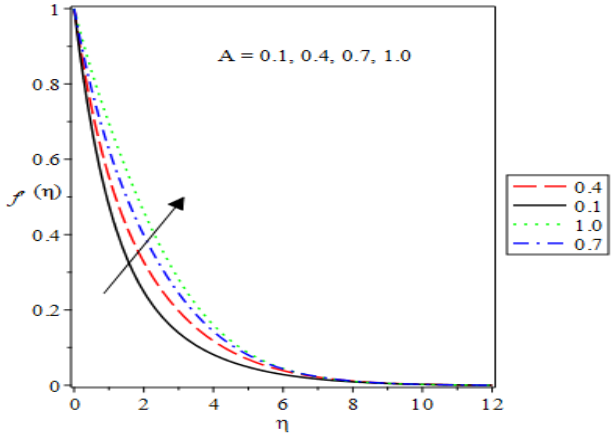

Figure 24. Effect of A on $f'(\eta)$

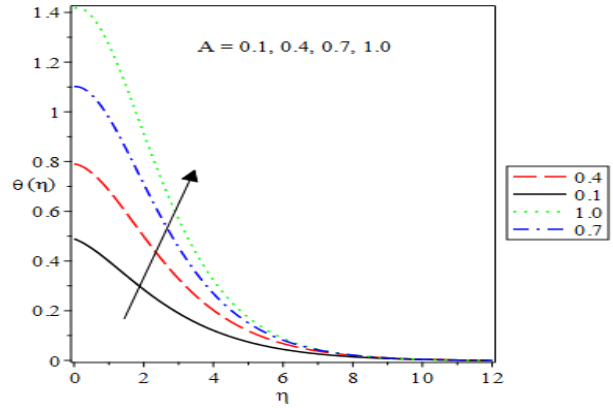

Figure 25. Effect of A on $\theta(\eta)$

The effect of the viscous dissipation parameter (Ec) on temperature is shown in Figure 27. This parameter, a fundamental factor governing momentum and heat transfer across various scientific and engineering domains, quantifies the conversion of kinetic energy into thermal energy due to viscous forces within a fluid. An increase in Ec indicates that a greater portion of the fluid's kinetic energy is transformed into heat, raising the fluid's temperature. This phenomenon is particularly significant in high-velocity or highly viscous flows, where frictional effects are pronounced.

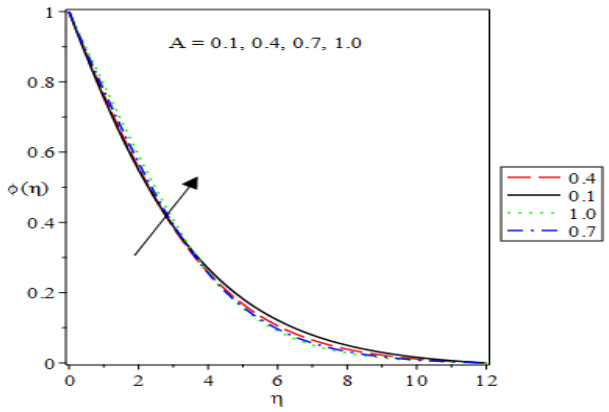

Figure 26. Effect of A on $\phi(\eta)$

Studies have shown that higher viscous dissipation leads to elevated temperature profiles within the fluid. In heat exchangers, Ec influences flow regimes (laminar or turbulent), affecting heat transfer rates: higher viscosity dampens fluid motion, reducing convective efficiency, while lower viscosity enhances mixing and thermal performance. In nuclear reactors, it affects coolant flow around fuel rods, impacting heat removal and pressure drops, which are critical for maintaining safe operating conditions under varying thermal loads. In thermal science, Ec shapes the interplay between viscous forces and thermal diffusion, guiding the analysis of boundary-layer behavior and heat dissipation in diverse systems.

In nanotechnology, it influences the dynamics of nanofluids and thin films, where viscous dissipation modulates thermal conductivity and energy transport at micro- and nanoscales, affecting device efficiency. In manufacturing, such as in polymer extrusion or metal casting, Ec governs flow behavior and heat transfer during material shaping, determining product quality, and energy usage.

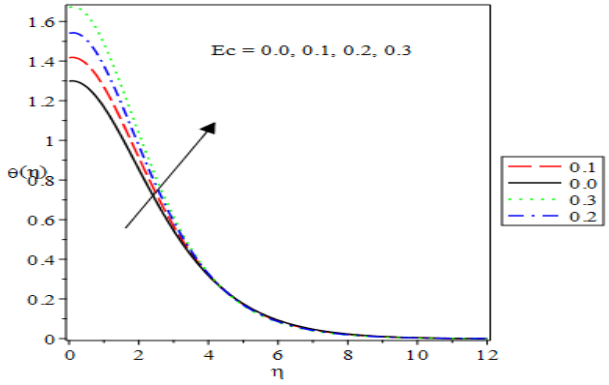

Figure 27. Effect of Ec on $\theta(\eta)$

In biomedical engineering, it is key to understanding blood flow in vessels or biofluid interactions in tissue scaffolds, where temperature- or shear-dependent viscosity impacts heat distribution and nutrient delivery. Across these fields, the viscous dissipation parameter bridges fluid mechanics and thermal performance, driving optimized design and functionality.

The Schmidt number (Sc), defined as the ratio of momentum diffusivity (viscosity) to mass diffusivity ($Sc = \frac{V}{D}$), is a dimensionless parameter that measures the relative thickness of the velocity and concentration boundary layers, playing a pivotal role in mass transfer processes across various scientific and engineering domains.

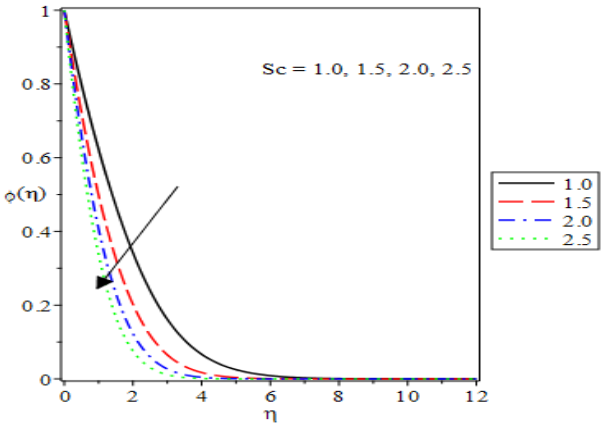

Figure 28. Effect of Sc on $\phi(\eta)$

An increase in Sc indicates that momentum diffusivity is high relative to mass diffusivity, resulting in a thinner concentration boundary layer compared to the velocity boundary layer. This thinner concentration boundary layer creates steeper concentration gradients near surfaces, enhancing mass transfer rates and reducing species concentration within the boundary layer [54], as shown in Figure 28. In heat exchangers, a high Schmidt number (e.g., in viscous fluids with low mass diffusivity) indicates slower species diffusion relative to momentum, affecting the efficiency of mass transfer in processes such as gas absorption or chemical reactions, which are crucial for exchanger performance.

In nuclear reactors, Sc influences the transport of radioactive species or corrosion products in

coolant flows, impacting contamination distribution and material integrity, particularly in systems with complex fluid chemistries. In thermal science, it is essential for modeling coupled heat and mass transfer, providing insights into diffusion-dominated phenomena in gases or liquids under thermal gradients. In nanotechnology, Sc governs nanoparticle dispersion in fluids, critical for applications such as drug delivery or sensor fabrication, where precise control of species concentration enhances functionality.

In manufacturing, such as in coating or polymerization, it affects the reactant diffusion rates, determining product uniformity and process efficiency. In biomedical engineering, Sc applies to biofluid dynamics, such as oxygen or nutrient diffusion in blood or tissues, where a higher value can slow mass transfer, influencing metabolic rates or therapeutic outcomes. Across these fields, the Schmidt number links fluid mechanics with mass transport, guiding the optimization of systems involving diffusion and convection.

The effect of the Prandtl number (Pr) on temperature is shown in Figure 29. Defined as the ratio of momentum diffusivity (viscosity) to thermal diffusivity, it (dimensionless parameter) significantly influences heat and mass transfer processes across various scientific and engineering fields by characterizing the relative thickness of velocity and thermal boundary layers in fluid flow. An increase in Pr indicates that the thermal boundary layer is thinner than the velocity boundary layer, enhancing the temperature gradient near the surface and improving heat transfer between the fluid and the surface.

Consequently, [55] noted that the fluid's temperature decreases more rapidly as it approaches thermal equilibrium with the surface. In heat exchangers, a high Prandtl number (e.g., in oils) indicates slower thermal diffusion relative to momentum, reducing heat transfer efficiency, whereas a low Pr (e.g., in liquid metals) enhances thermal performance, which is vital for compact designs. In nuclear reactors, Pr affects coolant behavior, particularly in sodium-cooled systems, where its low value improves heat removal from fuel rods, optimizing thermal management and safety.

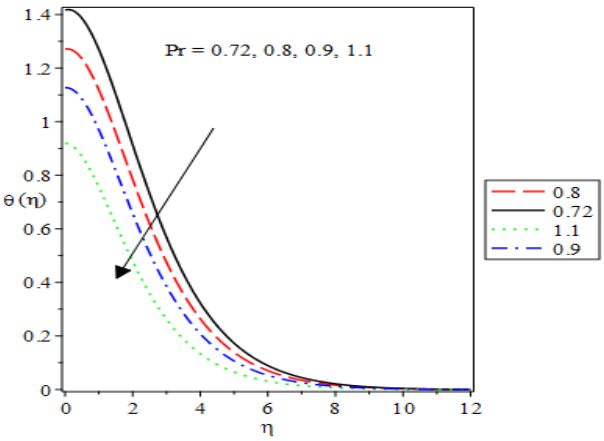

Figure 29. Effect of Pr on $\theta(\eta)$

In thermal science, the Prandtl number is essential for modeling convection, determining how heat propagates in fluids under varying temperature gradients, which is crucial for both theoretical and applied studies. In nanotechnology, Pr governs heat transfer in nanofluids or thin films, where tailored Pr values can enhance thermal conductivity or control energy dissipation in nanoscale devices.

In manufacturing, such as in polymer flows or metal solidification, Pr influences the interplay between viscous flow and heat transfer, affecting material properties and production rates. In biomedical engineering, Pr applies to biofluids such as blood, where variations in Pr due to temperature or composition distribution in tissues during thermal therapies or organ preservation is impacted. Thus, the Prandtl number serves as a critical link between fluid dynamics and thermal behavior, shaping system performance across these disciplines.

The impact of the thermophoresis parameter on species concentration is shown in Figure 30. An increase in this parameter reduces species concentration because thermophoresis induces a force that drives particles or molecules from regions of higher temperature toward cooler regions in a fluid.

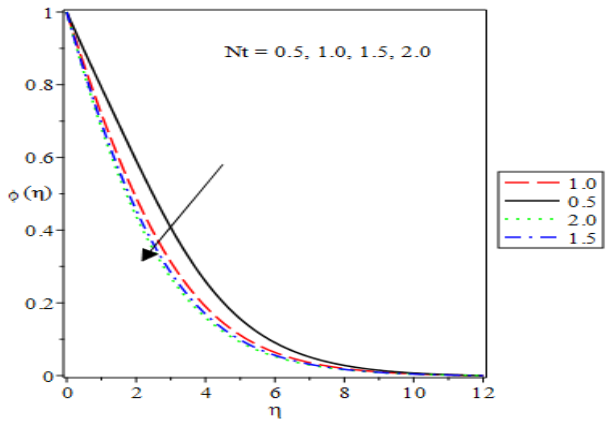

Figure 30. Effect of Nt on $\phi(\eta)$

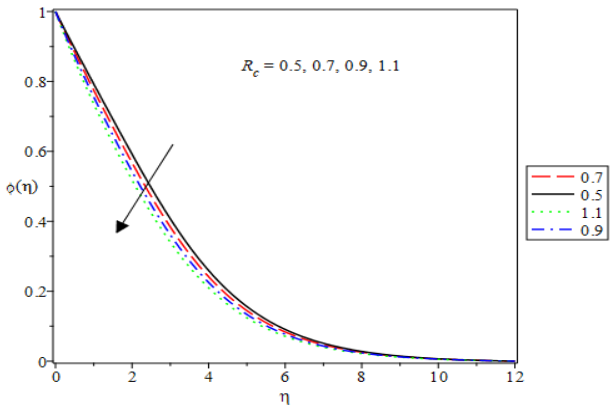

Figure 31. Effect of R_c on $\phi(\eta)$

In microfluidic or nanofluidic systems, where temperature gradients are significant, the thermophoresis parameter quantifies the strength of this thermally driven migration. As the parameter increases, the thermophoretic force strengthens, causing more particles or species to move away from hotter regions, typically near a heated surface, such as a stretching plate or microchannel wall. This migration decreases the local species concentration in the warmer region, as particles are transported to areas of lower temperature, resulting in reduced species concentration near the heat source. This effect is particularly pronounced in systems with non-Newtonian fluids or nanofluids, where temperature-dependent properties and boundary-layer dynamics further influence species distribution.

Figure 31 illustrates the effect of the kinetic parameter (R_c), on species concentration. An increase in R_c accelerates the chemical reaction rate within the fluid, leading to faster consumption of reactants and, consequently, a decrease in their concentration. This parameter quantifies the reaction rate, governing how quickly reactants are transformed into products through processes such as decomposition or recombination.

A higher R_c indicates a more rapid transformation, reducing the concentration of reactant species in the flow field, as they are consumed faster than they are replenished by diffusion or convection. This has significant implications in several areas: in combustion, where a higher reaction rate enhances energy release but may deplete fuel concentration, affecting flame stability; in pollutant dispersion, where faster reactions can reduce harmful species but alter flow chemistry; and in biological flows, where reaction rates influence nutrient or drug concentrations, impacting processes such as tissue oxygenation or drug delivery efficiency.

The Prandtl number, (Pr) defined as the ratio of momentum diffusivity to thermal diffusivity, significantly affects heat transfer characteristics. As Pr increases, the fluid's thermal diffusivity decreases, causing heat to diffuse more slowly compared to momentum. This leads to a thinner thermal boundary layer, and a steeper temperature gradient at the surface and higher local heat transfer rates, as indicated by $-\theta'(0)$ in Table 1. Results from [56] and the present study confirm this trend: as Pr increases from 1.0 to 4.0, the thermal gradient increases due to stronger localization of thermal effects near the surface. Similarly, an increase in the Schmidt number (Sc) reduces mass diffusivity, resulting in a thinner concentration boundary layer and an enhanced local mass transfer rate, quantified by $-\emptyset'(0)$, which is proportional to the Sherwood number. Table 1 shows that as Sc increases from 0.1 to 1.0, both [56] and the present study observe a significant increase in $-\emptyset'(0)$, indicating more efficient mass transfer at higher Sc.

This reflects the physical reality that lower mass diffusivity (higher Sc) intensifies concentration gradients at the surface, enhancing diffusive flux. However, the present study reports slightly lower values of $-\emptyset'(0)$ compared to [56] at $Sc = 0.1$, but the values align more closely at $Sc = 1.0$, suggesting improved agreement in mass transfer predictions at higher Schmidt numbers. Thus, the current results and previously published solutions, as compared in Table 1, demonstrate good agreement. This agreement validates the current solutions, as shown in Table 1.

Table 1. Effects of Pr on $-\theta'(0)$ and Sc on $-\emptyset'(0)$ When other parameters are fixed

Pr	Abbas et al. [51] $-\theta'(0)$	Present Study $-\theta'(0)$	Sc	Abbas et al. [51] $-\emptyset'(0)$	Present Study $-\emptyset'(0))$
1.0	0.1069591	0.2488867	0.1	0.2339228	0.1484306
4.0	0.0394994	0.0479404	1.0	0.6222070	0.5261632
7.0	0.0998794	0.0865925	-	-	-

5. Conclusion

The analysis of flexibility and nonlinear shear dilution/enhancement flow in a microfluidic heat transfer system is studied to evaluate thermal transfer performance. This analysis has revealed significant insights into optimizing thermal performance in microfluidic heat transfer systems. Flexible designs enhance flow modulation, improving heat transfer efficiency under varying conditions. Nonlinear shear dilution and enhancement flows enable precise control of thermal gradients. These findings highlight the importance of adaptive materials and flow dynamics in microfluidic applications. Future research should focus on scaling these systems for broader industrial use. The study underscores the potential for energy-efficient thermal management in compact devices. Overall, integrating flexibility and nonlinear flow mechanisms paves the way for advanced microfluidic technologies. The key results are as follows:

(1) An increase in variable fluid property $(A = 0.1, 0.4, 0.7, 1.0)$ enhances velocity, temperature, and concentration distributions. This improves heat transfer efficiency in microelectronics, enabling better cooling of compact, high-power devices and preventing thermal failure. In aerospace, these enhancements facilitate effective thermal management in confined spaces, improving component reliability and performance under extreme conditions.

(2) An increase in the volumetric heat source parameter $(\Delta_H = 0.0, 0.10, 0.13, 0.15)$ amplifies the velocity, temperature, and concentration distributions in nanofluids, enhancing heat dissipation in microelectronics. This helps maintain the performance and longevity of densely packed circuits under high thermal loads. In aerospace, it boosts thermal regulation in compact systems, ensuring reliability in harsh environments. However, elevated velocity and concentration may increase pressure losses and nanoparticle agglomeration risks, potentially challenging system efficiency and requiring careful design optimization in both domains.

(3) An increase in the shear enhancement parameter $(n = 2.0, 3.0, 4.0, 5.0)$ heightens concentration distribution in nanofluids, potentially improving heat transfer in microelectronics by enhancing cooling efficiency for high-density circuits.

(4) An increase in the Robin boundary term, $(C = 0.1, 0.2, 0.3, 0.4)$ which governs convective heat transfer at boundaries, decreases the temperature distribution in nanofluids. This enhances cooling efficiency in microelectronics by reducing the thermal stress on compact circuits and improving device reliability. In aerospace, it facilitates better thermal regulation in high-heat environments, ensuring component longevity under extreme conditions.

(5) An increase in the stretching parameter ($N = 0.5, 0.7, 0.9, 1.1$) which influences surface-driven flow, boosts velocity distribution in nanofluids. This enhances convective heat transfer in microelectronics, improving the cooling of high-density circuits and preventing overheating.

(6) An increase in flow orientation $\left(\gamma = 0^{\circ}, \frac{\pi}{10}, \frac{\pi}{6}, \frac{\pi}{9}\right)$ and flexibility parameters ($P = 0.0, 0.2, 0.4, 0.6$) reduces velocity distribution while elevating temperature and concentration distributions in nanofluids. This may compromise cooling efficiency in microelectronics by limiting fluid movement, potentially leading to localized overheating in dense circuits. Hence, it's proper to reduce the values of both parameters to maintain an appropriate temperature in microelectronics and other microfluidic heat transfer devices for efficient performance and durability.

Article Information Form

Acknowledgments
Authors would like to thank Professor Emeka Amos for his contributions.

Authors' Contribution
Conceptualization, U.A.; methodology, U.A.U., E.E., J.O.E., G.K.; software, U.A.U., E.E., J.O.E., G.K; validation, U.A.U., E.E., J.O.E.,G.K..; formal analysis, U.A.U., E.E., J.O.E.; investigation, U.A.U., E.E., J.O.E., G.K..; resources, U.A.U., E.E., J.O.E., G.K..; data curation, U.A.U., and G.K.; writing—original draft preparation, U.A.U., E.E.; writing—review and editing, U.A.U., E.E., G.K., J.O.E.; visualization, U.A.U., E.E., G.K.; supervision, U.A.U.; All authors have read and agreed to the published version of the manuscript.

The Declaration of Conflict of Interest/ Common Interest
No conflict of interest or common interest has been declared by authors.

Artificial Intelligence Statement
No artificial intelligence tools were used while writing this article.

References

[1] J. C. Maxwell, "A Treatise on Electricity and Magnetism," 3rd Edition, Clarendon Press, Oxford, UK, 1891.

[2] R. L. Hamilton, O. K. Crosser, "Thermal conductivity of heterogeneous two-component systems," Industrial and Engineering Chemistry Fundamentals, vol.1, pp. 187–191, 1962.

[3] C. Kleinstreuer, Y. Feng, "Experimental and theoretical studies of nanofluid thermal conductivity enhancement: A review," Nanoscale Research Letters, vol. 6, no. 1, p. 229, 2011.

[4] S. Ozerinc, S. Kakac, A. Guvenc, Y. Yazicioglu, "Enhanced thermal conductivity of nanofluids: A state-of-the-art review," Microfluidics and Nanofluidics, vol. 8, pp. 145–170, 2010.

[5] J. Fan, L. Wang, "Review of heat conduction in nanofluids," American Society of Mechanical Engineers' Journal of Heat Transfer, vol. 133, 040801, pp. 1–14, 2011.

[6] S. M. S. Murshed, K. C. Leong, C. Yang, "Thermophysical and electrokinetic properties of nanofluids: A critical review," Applied Thermal Engineering, vol. 28, pp. 2109–2125, 2008.

[7] E. V. Timofeeva, W. Yu, D. M. France, D. Singh, J. L. Routbort, "Nanofluids for heat transfer: An engineering approach," Nanoscale Research Letters, vol. 6, no. 1, p. 182, 2011.

[8] S. K. Das, S. U. S. Choi, W. Yu, T. Pradeep, "Nanofluids: Science and Technology," John Wiley & Sons, Inc., Publication, New Jersey, USA, 2008.

[9] D. Li, "Encyclopedia of Microfluidics and Nanofluidics," Springer, Amsterdam, Berlin, 2008.

[10] C. S. Kumar, "Microfluidic Devices in Nanotechnology: Applications," John Wiley & Sons, Inc., Publication, Hoboken, New Jersey, 2010.

[11] B. C. Pak, Y. I. Cho, "Hydrodynamic and heat transfer study of dispersed fluids with submicron metallic oxide particles," Experimental Heat Transfer, vol. 11, no. 2, pp. 151-170, 1998.

[12] Y. Xuan, W. Roetzel, "Conceptions for heat transfer correlation of nanofluids," International Journal of Heat and Mass Transfer, vol. 43, pp. 3701–3707, 2000.

[13] D. Wen, Y. Ding, "Experimental investigation into convective heat transfer of nanofluids at the entrance region under laminar flow conditions," International Journal of Heat Mass Transfer, vol. 47, pp. 5181–5188, 2004.

[14] S. Z. Heris, M. N. Esfahany, G. Etemad, "Investigation of CuO/water nanofluid laminar convective heat transfer through a circular tube," Journal of Enhanced Heat Transfer, vol. 13, pp. 279–289, 2006.

[15] S. Z. Heris, M. N. Esfahany, S. Gh. Etemad, "Experimental investigation of convective heat transfer of Al_2O_3/water nanofluid in circular tube," International Journal of Heat Fluid Flow, vol. 28, pp. 203–210, 2007.

[16] J. Buongiorno, "Convective transport in nanofluids," American Society of Mechanical Engineers' Journal of Heat Transfer, vol. 128, pp. 240–250, 2006.

[17] J. Y. Jung, H. S. Oh, H. Y. Kwak, "Forced convective heat transfer of nanofluids in microchannels," International Journal of Heat and Mass Transfer, vol. 52, pp. 466–472, 2009.

[18] U. Rea, T. McKrell, L. Hu, J. Buongiorno, "Laminar convective heat transfer and viscous pressure loss of alumina-water and zirconia-water nanofluids," International Journal of Heat and Mass Transfer, vol. 52, pp. 2042–2048, 2009.

[19] P. S. Vajjha, D. K. Das, D. P. Kulkarni, "Development of new correlations for convective heat transfer and friction factor in turbulent regime for nanofluids," International Journal of Heat and Mass Transfer, vol. 53, pp. 4607–4618, 2010.

[20] R. H. Khiabani, Y. Joshi, C. K. Aidun, "Heat transfer in microchannels with suspended solid particles: Lattice-Boltzmann based computations," American Society of Mechanical Engineers' Journal of Heat Transfer, vol. 132, 041003, pp. 1–9, 2010.

[21] M. Hojjat, S. Gh. Etemad, R. Bagheri, J. Thibault, "Convective heat transfer of non-Newtonian nanofluids through a uniformly heated circular tube," International Journal of Thermal Science, vol. 50, pp. 525–531, 2011.

[22] M. H. Fard, M. N. Esfahany, M. R. Talaie, "Numerical study of convective heat transfer of nanofluids in a circular tube two-phase model versus single-phase model," International Communications in Heat and Mass Transfer, vol. 37, pp. 91–97, 2009.

[23] R. Lotfi, Y. Saboohi, A. M. Rashidi, "Numerical study of forced convective Heat transfer for nanofluids: Comparison of different approaches," International Communications in Heat and Mass Transfer, vol. 37, pp. 74–78, 2010.

[24] M. M. Heyhat, F. Kowsary, "Effect of particle migration on flow and convective heat transfer of nanofluids flowing through a circular pipe," American Society of

Mechanical Engineers' Journal of Heat Transfer, vol. 132, 062401, pp. 1-9, 2010.

[25] A. Akbarinia, M. Abdolzadeh, R. Laur, "Critical investigation of heat transfer enhancement using nanofluids in microchannels with slip and non-slip flow regimes," Applied Thermal Engineering, vol. 31, pp. 556–565, 2011.

[26] S. Kondaraju, E. K. Jin, J. S. Lee, "Effect of the multi-sized nanoparticle distribution on the thermal conductivity of nanofluids," Microfluidics and Nanofluidics, vol. 10, pp. 133–144, 2011.

[27] J. H. Werth, M. Linsenmayer, S. M. Dammer, Z. Farkas, H. Hinichsen, K. E. Wirth, D.E. Wolf, "Agglomeration of charged nanopowders in suspensions," Powder Technology, vol. 133, pp. 106–112, 2011.

[28] W. Jiang, G. Ding, H. Peng, H. Hu, "Modeling of nanoparticles aggregation and sedimentation in nanofluid," Current Applied Physics, vol. 10, pp. 934–941, 2011.

[29] W. Evans, R. Prasher, J. Fish, P. Meakin, P. Phelan, P. Keblinski, "Effect of aggregation and interfacial thermal resistance on thermal conductivity of nanocomposites and colloidal nanofluids," International Journal of Heat and Mass Transfer, vol. 51, pp. 1431–1438, 2008.

[30] J. Li, C. Kleinstreuer, "Entropy generation analysis for nanofluid flow in microchannels," American Society of Mechanical Engineers' Journal of Heat Transfer, vol. 132, 122401, pp. 1-8, 2010.

[31] P. K. Singh, K. B. Anoop, T. Sundararajan, S. K. Das, "Entropy generation due to flow and heat transfer in nanofluids," International Journal of Heat and Mass Transfer, vol. 53, pp. 4757–4767, 2010.

[32] M. Kalteh, A. Abbassi, M. Saffar-Avval, J. Harting, "Eulerian-Eulerian two-phase numerical simulation of nanofluid laminar forced convection in a microchannel," International Journal of Heat and Fluid Flow, vol. 32, pp. 107–116, 2011.

[33] A. J. Omowaye, A. I. Fagbade, A. O. Ajayi, "Dufour and Soret effects on steady MHD convective flow of a fluid in a porous medium with temperature-dependent viscosity: Homotopy analysis approach," Journal of the Nigerian Mathematical Society, 2015.

[34] R. C. Fernando, E. G. Hernandez-Martinez, R. D. J. Portillo-Velez, L. Rejón-García, "Nanotechnology Applications in Ground Heat Exchanger Pipes: A Review," Applied. Sciences, vol. 12, 3794, 2022.

[35] B. Wang, Y. Liu, L. Ling, "Nanofluid double diffusive natural convection in a porous cavity under multiple force fields," Numerical Heat Transfer, Part A: Applications, 2019.

[36] M. K. Virginia, T. T. M. Onyango, J. K. Kwanza, "Analysis of the Effect of Stretching Parameter and Time Parameter on MHD Nanofluid Flow in the Presence of Suction," Global Journal of Pure and Applied Mathematics, vol. 15, no. 5, pp. 637-648. 2019.

[37] N. K. Muhammad, F. M. Aldosari, Z. Wang, M. Yasir, M. Afikuzzamand, I. E. Elseesy, "Overview of solar thermal applications of heat exchangers with thermophysical features of hybrid nanomaterials," Nanoscale Advances., vol. 6, pp. 136-145, 2024.

[38] P. B. Reddy, "Radiation and chemical reaction effects on unsteady MHD free convection parabolic flow past an infinite isothermal vertical plate with viscous dissipation," International Journal of Applied Mechanics and Engineering, vol. 24, no. 2, pp. 343-358, 2019.

[39] Y. Menni, A. J. Chamkha, H. Ameur, "Advances of nanofluids in heat Exchangers: A review," Heat Transfer, pp. 1–29, 2020.

[40] H. A. Peker, F. A. Cuha, “Solving One-Dimensional Bratu's Problem via Kashuri Fundo Decomposition Method,” Romanian Journal of Physics, vol. 68, no. 5-6, p. 109, 2023.

[41] H. A. Peker, F. A. Cuha, “Application of Kashuri Fundo Transform and Homotopy Perturbation Methods to Fractional Heat Transfer and Porous Media Equations,” Thermal Science, vol. 26, no. .(4A), pp. 2877-2884, 2022.

[42] B. Peker, F. A. Cuha, H. A. Peker, “Analytical solution of Newton's Law of cooling equation via Kashuri Fundo transform,” Necmettin Erbakan University Journal of Science and Engineering, vol. 6, no. 1, 2024.

[43] H. A. Peker, F. A. Cuha, B. Peker, “Solving steady heat transfer problems via Kashuri Fundo transform,” Thermal Science, vol. 26, no. 4A, pp. 3011-3017, 2022. Doi:10.2298/TSCI2204011P.

[44] F. A. Cuha, H. A. Peker, “Solution of Abel's Integral Equation by Kashuri Fundo Transform,” Thermal Science, vol. 26, no. 4A, pp. 3003-3010, 2022.

[45] J. Boussinesq, “Analytical Theory of Heat,” Gauthier-Villars. Paris, 1877.

[46] A. K. A. Hakeem, G. Bhose, M. Y. A. Sait, V. G. Nagaraj, M. R. Muhammad, “Nonlinear Studies on the effect of non-uniform Heat Generation/Absorption on Hydromagnetic Flow of Nanofluid over a Vertical Plate,” Journal of Nonlinear Analysis, Modelling, and Control, vol. 22, no. 1, pp. 1-16, 2017.

[47] L. V. Woodcock, “Origins of shear dilatancy and shear thickening phenomena,” Chemical Physics Letters, vol. 111, no. 4–5, pp. 455–461, 1984. Bibcode:1984CPL.111.455W.

[48] P. A. Davidson, “Magnetic damping of ets and vortices,” Journal of Fluid Mechanics, vol. 299, pp. 153-186, 1995.

[49] J. A. Shercliff, “The flow of conducting fluids in circular pipes under transverse magnetic fields,” Journal of Fluid Mechanics, vol. 1, pp. 644-666, 1956.

[50] R. J. Rosa, “MHD energy conversion,” Institute of Electrical and Electronics Engineers Transactions on Power Apparatus and Systems, vol. 87, no. 8, pp. 1713-1722, 1968. McGraw-Hill.

[51] P. Johannes, D. G. Kröger, “Solar chimney power plant performance,” Journal of Solar Energy Engineering, vol. 128, no. 3, pp. 302-311, 2006.

[52] A. R. A. Khaled, K. Vafai, “The role of porous media modeling flow and heat transfer in biological tissues,” International Journal of Heat and Mass Transfer, vol. 46, pp. 4989-5003, 2003.

[53] P. Singh, A. K. Pandey, M. Kumar, “Forced convection in MHD slip flow of alumina-water nanofluid over a flat plate,” Journal of Enhanced Heat Transfer, vol. 23, no. 6, pp. 487–497, 2016.

[54] U. U. Awucha, A. Okechukwu, “A soret dissipation effect on heat and mass transmission of non-Newtonian casson radiative nanofluid flow with Lorentz drag and Rosseland radiation,” Journal of Pure and Applied Sciences, vol. 21, no. 2, pp. 120-127, 2022.

[55] A. U. Uchenna, E. Esekhaigbe, O. B. Inalu, “Analysis of boundary layer thickness and temperature distribution in a fluidic stream across a stretching sheet with thermal nonequilibrium and viscous heating effects," ElCezeri Journal of Science and Engineering, vol. 12, no. 2, pp. 134-152, 2025.

[56] A. Abbas, M. A. Shahid, A. Ilyas, M. B. Jeelan, “Effect of inclined magnetic field and thermal radiation on Williamson nanofluid flow and heat transfer along the stretching/shrinking wedge,” Journal of Nanofluids, vol. 12, pp. 2237-2244, 2023.